GA–A27397

QUIESCENT H-MODE OPERATION USING TORQUE FROM NON-AXISYMMETRIC, NON-RESONANT MAGNETIC FIELDS

by

K.H. BURRELL, A.M. GAROFALO, W.M. SOLOMON, M.E. FENSTERMACHER,
D.M. ORLOV, T.H. OSBORNE, J.-K. PARK, and P.B. SNYDER

OCTOBER 2012

GENERAL ATOMICS

GA–A27397

QUIESCENT H-MODE OPERATION USING TORQUE FROM NON-AXISYMMETRIC, NON-RESONANT MAGNETIC FIELDS

by
K.H. BURRELL, A.M. GAROFALO, W.M. SOLOMON,* M.E. FENSTERMACHER,†
D.M. ORLOV,‡ T.H. OSBORNE, J.-K. PARK,* and P.B. SNYDER

This is a preprint of a paper to be presented at the 24th IAEA Fusion Energy Conference, October 8–12, 2012, in San Diego, California and to be published in the *Proceedings.*

*Princeton Plasma Physics Laboratory, Princeton, New Jersey 08540-0451, USA.
†Lawrence Livermore National Laboratory, Livermore, California 94550-0808, USA.
‡University of California-San Diego, La Jolla, California 92093, USA.

Work supported by
the U.S. Department of Energy under
DE-FC02-04ER54698, DE-AC02-09CH11466,
DE-AC52-07NA27344, and DE-FG02-05ER54809

GENERAL ATOMICS PROJECT 30200
OCTOBER 2012

GENERAL ATOMICS

Quiescent H-mode Operation Using Torque from Non-axisymmetic, Non-resonant Magnetic Fields

K.H. Burrell 1), A.M. Garofalo 1), W.M. Solomon 2), M.E. Fenstermacher 3),
D.M. Orlov 4), T.H. Osborne 1), J.-K. Park 2), and P.B. Snyder 1)

1) General Atomics, P.O. Box 85608, San Diego, California 92186-5608, USA
2) Princeton Plasma Physics Laboratory, Princeton, New Jersey 08543-0451, USA
3) Lawrence Livermore National Laboratory, Livermore, California 94550-0808, USA
4) University of California-San Diego, La Jolla, California 92093, USA

e-mail contact of main author: burrell@fusion.gat.com

Abstract. Quiescent H-mode (QH-mode) sustained by magnetic torque from non-axisymmetric magnetic fields is a promising operating mode for future burning plasmas including ITER. Using magnetic torque from n=3 fields to replace counter-I_p torque from neutral beam injection, we have achieved long duration, counter-rotating QH-mode operation with NBI torque ranging continuously from counter-I_p up to co-I_p values of about 1 Nm. This co-I_p torque is about 3 times the scaled torque that ITER will have. This range also includes operation at zero net NBI torque, applicable to RF wave heated plasmas. These n=3 fields have been created using coils either inside or, most recently, outside the toroidal coils. Experiments utilized an ITER-relevant lower single-null plasma shape and were done with ITER-relevant values ν^*_{ped}~0.05, β^{ped}_T~1% and β_N=2. Discharges have confinement quality H_{98y2}=1.3, in the range required for ITER. Preliminary low q_{95}=3.4 QH-mode plasmas reached fusion gain values of $G=\beta_N H_{89}/q_{95}^2$=0.4, which is the desired value for ITER; the limits on G have not yet been established. The QH-mode work to date has made significant contact with theory. The importance of edge rotational shear is consistent with peeling-ballooning mode theory. We have seen qualitative and quantitative agreement with the predicted NTV torque.

1. Introduction

The promise of quiescent H-mode (QH-mode) as a viable operating regime for future burning plasma devices including ITER has been enhanced considerably in recent DIII-D experiments. These results were achieved [1,2] by maintaining strong edge counter-I_p rotation and rotation shear even when the neutral beam injection (NBI) torque is co-I_p by utilizing the counter-I_p torque due to neoclassical toroidal viscosity (NTV) produced by nonaxisymmetric, non-resonant n=3 magnetic fields. We have demonstrated stationary, QH-mode plasmas without edge localized modes (ELMs) with NBI torque levels ranging from counter-I_p through the zero torque expected in devices heated by radio frequency waves to modest co-I_p values exceeding the equivalent NBI torque levels expected in ITER. We produced these reactor relevant plasmas using n=3 fields from nonaxisymmetric coils either inside or, in the most recent experiments, outside the vacuum vessel and toroidal coils. In addition, QH-mode plasmas have simultaneously demonstrated the reactor requirements of stationary, constant density H-mode operation without ELMs at the maximum possible stable pedestal pressure and with particle transport rapid enough for helium exhaust [3,4]. Accordingly, QH-mode operation in future burning plasma devices can provide H-mode confinement levels (ITER H_{98y2}>1) while simultaneously eliminating the pulsed divertor heat loads due to ELMs.

QH-mode was originally discovered on DIII-D [5,6] and was subsequently investigated on JET [7], ASDEX-Upgrade [7,8], and JT-60U [9,10]. QH-modes in DIII-D have been run for long duration, a bit longer than 4 s, which is about 30 energy confinement times, τ_E, or about 2 current relaxation times τ_R [3]. The maximum duration to date has been limited by neutral beam pulse length. Once sufficient power is supplied to create QH-mode (typically 3 to 4 MW), the plasmas remain quiescent even at the input powers needed to reach the core beta limit (typically, 15 MW). QH-mode plasmas exhibit time-averaged edge particle transport more rapid than that produced by ELMs while operating at reactor-relevant pedestal beta (β^{ped}_T~1%) and collisionality (ν^*_i~0.05) [4,11]. QH-mode is a robust operating regime which has been seen over the entire range of triangularity ($0.16 \leq \delta \leq 0.82$) and safety factor, q_{95} ($3.4 \leq q_{95} \leq 8.5$), explored to date. There are no specific q_{95} values required for ELM-free operation, unlike RMP ELM suppression [12,13]. QH-modes operate with constant density and radiated power, unlike the ELM-free plasmas created in NSTX using lithium wall coating [14]. An example of a long pulse QH-mode plasma is shown in Fig. 1.

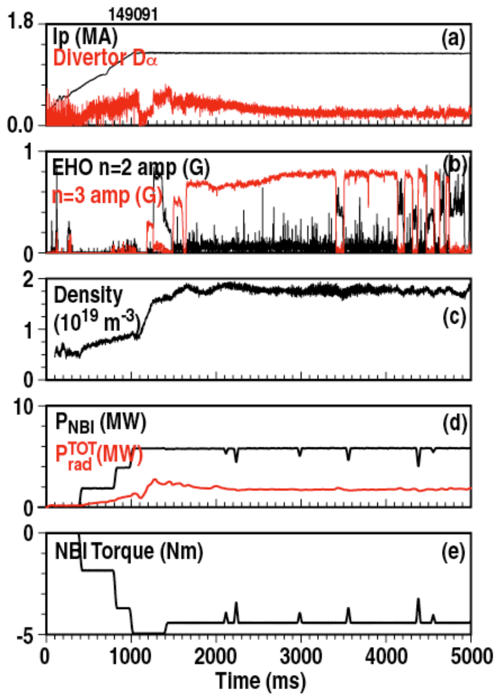

Fig. 1. Long-pulse QH-mode with counter-I_p NBI. (a) Plasma current and divertor D_α emission, (b) edge magnetic field from the n=2 and n=3 harmonics of the EHO, (c) line-averaged density, (d) NBI power and total radiated power, and (e) neutral beam torque (negative is counter-I_p). Toroidal field is 2.0 T.

QH-mode plasmas operate near but below the peeling-ballooning mode stability boundary that sets the ELM limit [4,15,16]. The additional transport from an edge MHD mode, the edge harmonic oscillation (EHO), provides the extra particle transport that allows a transport equilibrium at conditions just below the peeling boundary. The enhanced particle transport is illustrated in Fig. 1 by the increase in the divertor D_α emission when the EHO turns on around 1300 ms. Theory predicts that the EHO is a kink-peeling mode that is destabilized by edge rotational shear at conditions just below the edge current limit which leads to explosive growth of the ELM [17]. Experimental results are consistent with the predicted importance of the edge rotational shear [1,2,4,16]. The theory predicts that QH-mode is possible with either co-I_p or counter-I_p edge rotation provided the shear in the edge rotation is sufficiently large. Although it is easier to create QH-mode with counter-I_p NBI, QH-mode has also been created with co-I_p NBI [4,16]. The 3.5 Nm NBI torque used in these co-injected discharges, when scaled to future devices, is far beyond that available in those machines. For example, using the scaling discussed by Garofalo et al. [1], in terms of the rotation produced, the 35 Nm torque available from the ITER neutral beams is equivalent to about 0.35 Nm NBI torque in DIII-D.

To demonstrate QH-mode operation with reactor relevant levels of co-I_p NBI torque, QH-mode in DIII-D must be sustained with NBI torque in the range of 0 to roughly 1 Nm. Work over the past three years has shown that NTV can provide the counter-I_p torque [1,2] needed to maintain the edge rotational shear. The present paper gives the latest results, highlighting low torque QH-mode operation using a nonaxisymmetric coil outside the toroidal coil. Such a coil configuration facilitates QH-mode operation on burning plasma devices where coils inside the vacuum vessel are difficult to engineer.

2. Investigations using low levels of co-I_p NBI torque

DIII-D has two sets of coils that can be used to correct intrinsic error fields and to create non-axisymmetric magnetic fields [2]. The C-coil is a set of six roughly rectangular coils, which are located outside the vacuum vessel and toroidal coil; the I-coil is a set of 12 coils located inside the vacuum vessel and, hence, inside the toroidal coil. For the experiments performed in 2012, the C-coil was connected to produce NTV torque using a field with toroidal mode number n=3, while the I-coil provided n=1 error field correction. In addition, we upgraded the power supply configuration to allow full 7.1 kA operation in the C-coil (up from 6.2 kA in previous years [2]). NTV torque calculations using a model by Park et al.

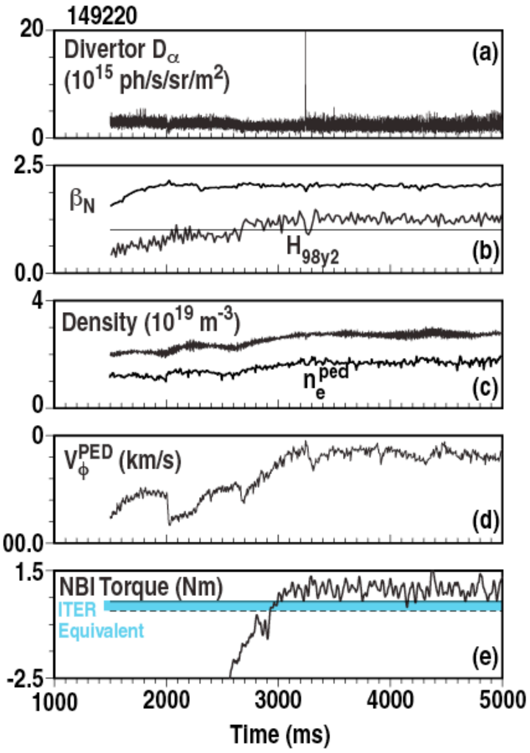

Fig. 2. QH-mode with co-I_p NBI torque using NRMF from C-coil at 7.1 kA. (a) Divertor D_α showing multisecond ELM-free operation, (b) ITER98(y,2) energy confinement time and normalized beta, (c) line-averaged and pedestal densities showing constant density operation without ELMs, (d) pedestal carbon toroidal rotatio (counter-I_p rotation is negative), (e) neutral beam torque. Shaded band in (e) shows the ITER torque scaled to DIII-D. Toroidal field is 1.8 T and q_{95} is 4.7.

to maintain the normalized plasma beta, β_N, at a fixed value independent of the input torque.

Using NTV torque from the C-coil only, stationary QH-mode operation is possible with reactor relevant co-I_p NBI torque levels as is shown in Fig. 2. QH-mode operation is possible with NBI torque both above and below the ITER equivalent co-I_p torque level [1]. These shots are free of ELMs, exhibit constant line averaged and pedestal densities, have counter-I_p pedestal rotation and operate with reactor relevant levels of energy confinement (H_{98y2}=1.3) and normalized beta (β_N=2).

A graphic illustration of the effect of the n=3 NRMF is given in Fig. 3 where we compare the carbon toroidal rotation profile for two shots, one with and one without the n=3 NRMF. As can be seen there, for similar [18,19] predict and experiments confirm that, with the present coil current limits, the C-coil can produce the greater NTV torque [2].

The theory of NTV indicates that it is the nonresonant magnetic field components that can produce significant torque. Vacuum field calculations show the non-axisymmetric n=3 fields used in the present experiments are primarily nonresonant magnetic fields (NRMFs) [2]. Although this vacuum field calculation ignores possible plasma response, recent calculations of that response demonstrate that it tends to reduce the resonant components of the field in the plasma [20]. The importance of the nonresonant field components is another difference between QH-mode with NRMFs and RMP ELM suppression [12,13].

To investigate the effects of changing NBI torque, we initiated the plasma discharge with predominantly counter-I_p NBI to create a QH-mode plasma and then we ramped the input NBI torque from that counter-I_p value towards co-I_p. The digital plasma control system (PCS) produced the torque ramp by altering the duty cycle of the co-I_p and counter-I_p neutral beams. It was also used to control the total NBI power

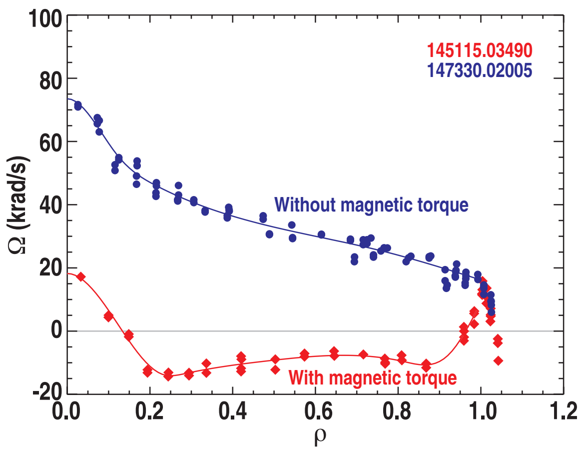

Fig. 3. NRMF significantly alters carbon toroidal rotation profiles for two QH-mode shots at approximately the same co-I_p NBI torque. Shot 145115 with NRMF, has plasma current 1.1 MA, toroidal field 1.9 T, q_{95} 5.2, β_N 2.1, NBI torque 1.7 Nm, and line averaged density 3.3×10^{19} m^{-3} while shot 147330 without NRMF has current 1.0 MA, toroidal field 2.0 T, q_{95} 5.4, β_N 1.8, NBI torque 1.8 Nm and density 2.4×10^{19} m^{-3}. To compensate for the difference in density, the rotation speed for 147330 has been multiplied by 0.7.

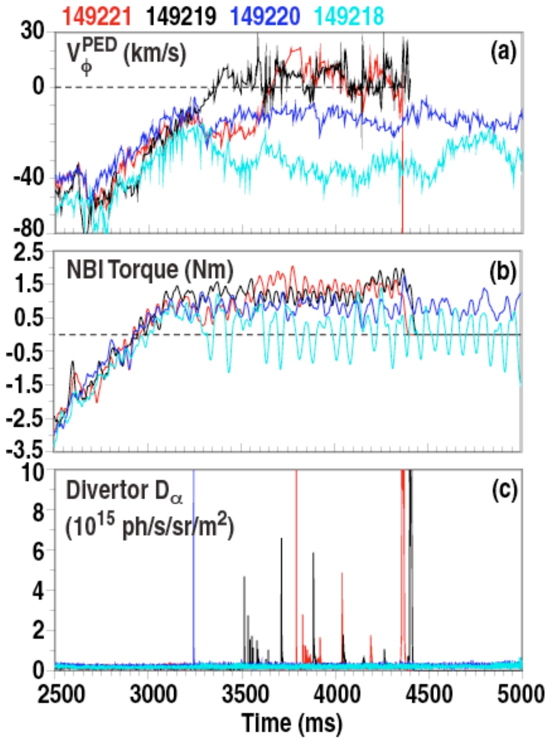

Fig. 4. Plot illustrating maximum co-I_p NBI torque which allows QH-mode operation. (a) Pedestal carbon toroidal rotation speed, (b) NBI torque, (c) Divertor D_α radiation. The magenta and blue curves show shots that had stationary QH-mode operation while the red and cyan curves show cases with slightly higher neutral beam input torque where the rotation diverges, indicating the NBI torque exceeds the peak NTV torque. Locked modes occur once the pedestal rotation crosses zero.

operation at zero net NBI torque is also quite straighforward. Accordingly, we have shown that we can operate QH-mode at NBI torque levels bracketing the scaled co-I_p NBI torque expected in ITER (0.35 Nm).

As will be discussed more in the next section, the theory of the NTV torque predicts the magnitude of the torque scales with $(\delta B)^2$, where δB is the perturbed field in the plasma. Since δB must be related to the current in the C-coil, we performed a test of this scaling by varying the C-coil current shot by shot while keeping the NBI torque fixed at zero, choosing C-coil current values so that the square of the current changed in the ratio 1:0.75:0.6:0.33:0.0. The surprising results of this scan are shown in Fig. 5. There is essentially no change in pedestal rotation until the square of the current was reduced by a factor of 3; even then, the change is

co-I_p NBI torques, the rotation with the NRMF is still in the counter-I_p direction while the rotation without NRMF is strongly co-I_p. Although the toroidal rotation is quite different, both shots are QH-mode and have similar shear in the edge toroidal rotation associated with the radial electric field, $\omega_e = E_r/RB_\theta$. Our recent results [1,2] indicate that it is this shear which is important in maintaining the EHO. The shot with NRMF is a marginal QH-mode; it has an NBI torque which is large enough that the shot has some ELMs. The shot has constant density and is ELM-free for about 200 ms during the time shown in Fig. 3.

To establish the co-I_p NBI torque limit for QH-mode operation for the discharges like the one shown in Fig. 2, we fired a series of shots, shown in Fig. 4, where we increased the co-I_p NBI torque during the 3000-5000 ms period. QH-mode operation was maintained for NBI torque levels at or below about 1 Nm. The maximum 1 Nm is 3 times the scaled ITER NBI torque level. As is shown in Fig. 5,

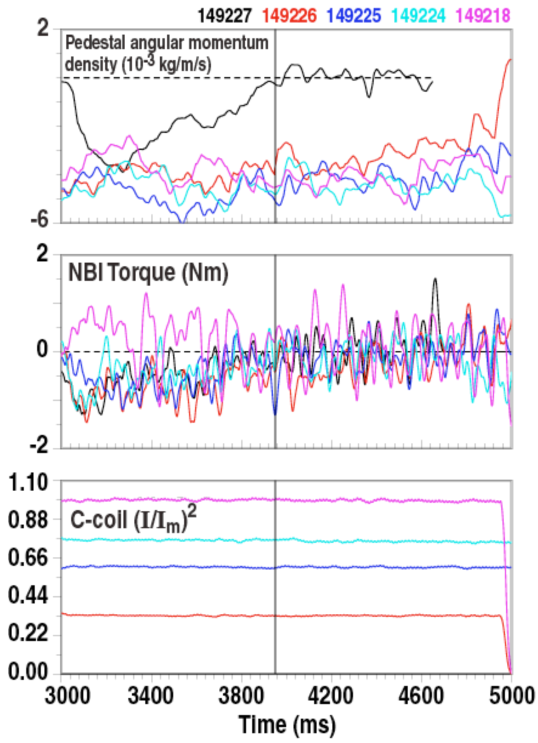

Fig. 5. Change in edge rotation as C-coil current is varied. (a) Pedestal angular momentum density $n_e m_d v_\phi$, (b) NBI torque, and (c) square of ratio of C-coil current to the maximum allowable current, 7.1 kA. Plotting $n_e m_d v_\phi$ compensates for small variations in density.

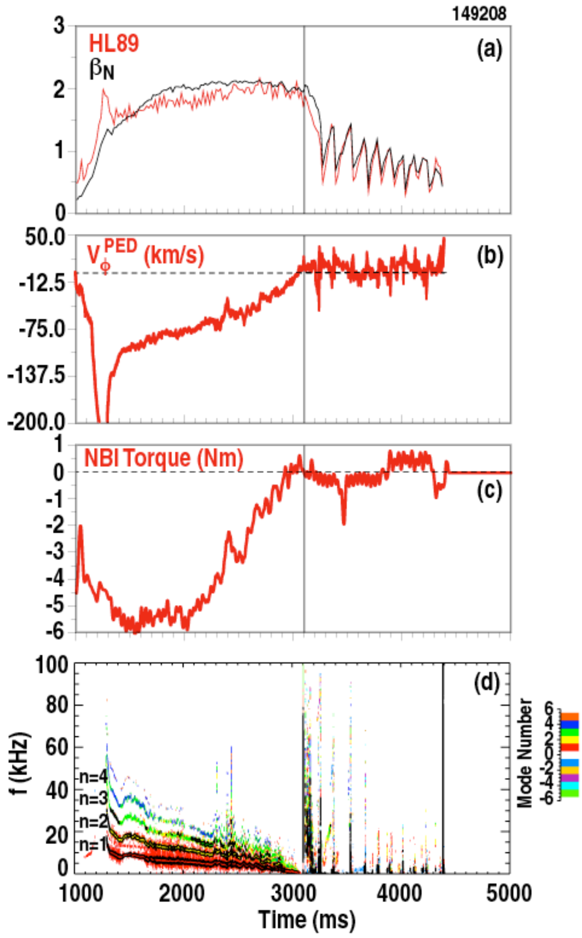

Fig. 6. With n = 1 EHO, low torque operation leads to mode locking. Locked mode onset time is shown by vertical bar. (a) Confinement relative to the ITER89 L-mode scaling and β_N show confinement drop after locked mode starts, (b) pedestal carbon toroidal rotation speed, (c) NBI torque, (d) frequency spectrum of the EHO. Plasma is lower single null divertor with 1.1 MA plasma current, 1.9 T toroidal field and q_{95} of 5.

minor. There was a substantial change when the C-coil current was turned off. Indeed, the plasma slowed and disrupted due to a locked mode. Coupling these observations with the peak co-I_p torque of about 1 Nm suggests that the variation of the NTV torque with rotation near ω_E=0 is very rapid.

In developing the discharges at reactor relevant torque over the past two years, we discovered a feature of the EHO that we had not appreciated before. If the EHO has a predominantly *n*=1 toroidal mode structure, the EHO itself can exert sufficient torque that, at low neutral beam torque, it can cause mode locking. An example of this is shown in Fig. 6, where the EHO frequency drops as the NBI torque becomes more co-I_p. Ultimately, the mode locks to the wall, confinement degrades markedly and the shot disrupts about 1500 ms later. In order to make the co-I_p torque shots run, we had to develop a means to eliminate the *n*=1 component of the EHO.

We do not have a complete theory which predicts the dominant toroidal mode number for the EHO for a given set of plasma conditions. We have established several different ways to change the toroidal mode number or the overall character of the EHO including changes in plasma current or edge safety factor q_{95}, changes in plasma shape (especially triangularity) and increase in the plasma density. At the highest densities reached in QH-mode plasmas, the coherent EHO disappears and broadband oscillation appears on the signals from the edge magnetic probes [2,3]. Furthermore, in our NRMF experiments in 2010 [1], we discovered that odd parity *n*=3 NRMF from the I-coil would reliably shift the EHO toroidal mode number from *n*=1 to *n*=3. At present, we do not have a theoretical explanation for this shift in mode number.

Over the past three years, we have used several of these techniques to suppress the *n*=1 EHO. In the 2010 campaign, all the QH-mode experiments with NRMF used odd parity *n*=3 fields from the I-coil, which automatically eliminated the *n*=1 EHO. After finding in 2011 that the *n*=1 component of the EHO was detrimental at low NBI torque, we slightly changed the plasma shape to alter the divertor cryopumping and increase the density; this allowed us to access the broadband MHD [2]. In the present campaign, we used this density control plus a toroidal field ramp during the shot to alter q_{95} and again obtained the broadband MHD. An example of the frequency spectrum of this is shown in Fig. 7.

We have performed peeling-ballooning stability calculations, shown in Fig. 8, for the discharges with NRMF using the technique employed previously [4,15,16]. Within the error

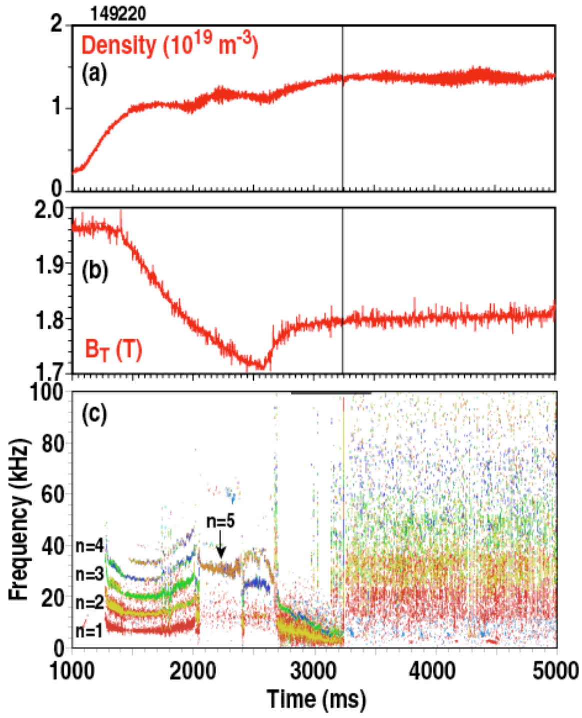

Fig. 7. Toroidal field alteration and density increase were used to suppress the n=1 EHO and obtain broadband edge MHD. (a) line averaged density, (b) toroidal field and, (c) frequency spectrum of the Mirnov probe signals. The coherent, n=1 EHO is gone by 2000 ms and even the coherent n=2 and n=4 modes are eliminated by 3250 ms.

bars, the operating point for the discharge with NRMF from the C-coil alone is on the peeling boundary; this is similar to the operating point of QH-mode discharges without NRMF [4,15,16] and to the operating points of the discharges which used combinations of the C-coil and I-coil [2,3].

We have also used the present C- and I-coil configuration to perform experiments on low q_{95} discharges to determine how high the fusion gain parameter $G=\beta_N H_{89}/q_{95}^2$ can be in QH-mode plasmas. We used a more aggressive toroidal field ramp than in Fig. 7 to lower q_{95} to 3.4. Our best result to date is G=0.4 [2]. This is a very preliminary result and considerable work still remains to be done in this area.

3. Comparison with Theory of NTV torque

The theory of NTV torque [21-23] was applied first to stellarators where the large field variations produce the dominant effects on the plasma rotation. In the present tokamak case where the field perturbations $\delta B/B$ are of order 10^{-3}, the NTV torque is just one of several factors that influence the rotation. The rate of change of the angular momentum due to the NTV torque can be expressed as [24]

$$\left.\frac{\partial\left\langle\rho_m R^2\Omega\right\rangle}{\partial t}\right|_{\mathrm{NTV}} = -\rho_m\mu_{\parallel}\left(\Omega,\ \nu_i\right)\left(\frac{\delta B_{3D}}{B_0}\right)^2\left(\left\langle R^2\Omega\right\rangle-\left\langle R^2\Omega_{\mathrm{NTV}}\right\rangle\right)\quad . \tag{1}$$

Here, $\Omega=V_\phi/R$ is the angular rotation speed, $\rho_m=nm_i$ is the mass density, ν_i is the ion collision frequency, and $\mu_\parallel$ is a viscosity coefficient. The right hand side of Eq. (1) is the torque density due to NTV.

There are three important features of the expression on the right hand side of Eq. (1). First, the NTV torque density is zero at the so-called neoclassical offset velocity $V^{NTV}=R\Omega_{NTV}$, which is in the counter-I_p direction. This counter-I_p offset velocity has been seen experimentally [25]. Second, for rotation speeds $V_\phi>V^{NTV}$, the NTV torque is in the counter-I_p direction. Third, the viscosity coefficient $\mu_\parallel$ has a local peak at $\omega_E=0$.

This local peak in $\mu_\parallel$ allows us to understand the sudden jump in the pedestal rotation, which occurs in the present experiments when the NBI torque is increased too far. This jump is seen in Fig. 4(a) and has also been seen in similar experiments in 2011 [2]. Given a localized peak in the NTV torque, if the other torque input to the plasma is increased from counter-I_p towards co-I_p by increasing the NBI torque, the rotation will gradually walk up the left hand side of the NTV peak. When the sum of the other torques gets large enough, the rotation should suddenly jump to a much more co-I_p value. This jump is what is seen

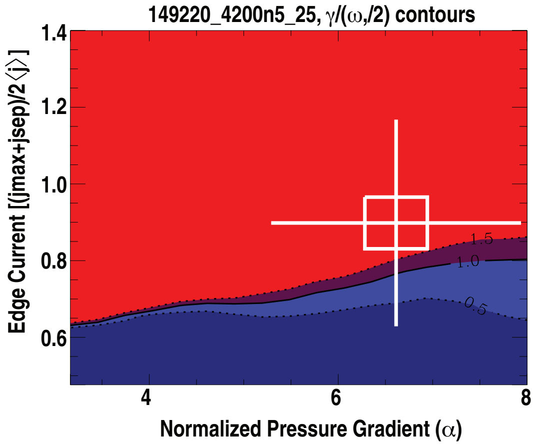

Fig. 8. Peeling ballooning stability result. Horizontal axis is normalized pedestal pressure gradient (MHD alpha parameter); vertical axis is peak edge current density normalized by twice the volume averaged current density. Plasma operating point is shown by the box with error bars. Stable region is blue; unstable region is red. Note suppressed zero on both axes.

experimentally. The jump in the actual experiment is not as large as the NTV theory would suggest because locked modes limit the rotation excursion. Accordingly, the presence of the jump is consistent with NTV theory, although the overall rotation evolution is determined by more than the NTV torque.

Quantitative comparisons have been made between NTV torque predictions and the NTV torque determined experimentally [1,2]. These were made by first calculating the internal magnetic field in the plasma using the IPEC code [18] and then using this result in a separate neoclassical code [19] which evaluates the NTV torque. The agreement between the predictions and the measurements was quite good.

The C-coil current scan results in Fig. 5, however, present a significant puzzle, since it appears that we get sufficient torque to maintain edge counter rotation even when we reduce the square of the C-coil current by a factor of 3. This shot at reduced C-coil current is consistent with the net zero NBI torque operation that we obtained with the I-coil alone in 2010 [2]. Using the IPEC+NTV prediction of a factor of two less torque from the I-coil than the C-coil at the same current and the theoretical prediction that the torque should scale as the current squared, shot 149226 in Fig. 5 and shot 141439 [2] have the same NTV torque. Indeed, both of them are long duration QH-modes that operate with zero net NBI torque.

The theory of NTV torque indicates that the peak in $\mu_{||}$ at ω_E=0 is quite sharp [23,24]. Previous experimental measurements looking at rotation in the plasma core around ρ=0.6 indicated that the peak is somewhat broader than theory could easily accommodate [23,24]. In the present experiments, direct measurements show an ω_E=0 region at the top of the H-mode edge pedestal which is at least 4 cm wide for the shots in Fig. 5 with nonzero C-coil current. This is also the location where the rotation speeds plotted in Fig. 5 are measured. The results in Fig. 5 are consistent with the sharp $\mu_{||}$ peak predicted theoretically.

4. Extrapolations to ITER

In order to determine whether QH-mode operation is possible in ITER, two key questions need to be answered. The first is whether the H-mode edge in ITER will operate at near the peeling boundary in the ELM stability diagram, since all QH-modes created to date in other machines operate on that boundary. Calculations using the EPED1 model [26] have been carried out to determine the pedestal parameters for various pedestal densities in ITER; these were then used by the ELITE [27] code to determine the stability diagram [2]. As is discussed in Ref. [2], when the pedestal densities are in the range 2×10^{19} m^{-3} to 1.2×10^{20} m^{-3}, the ITER plasma will operate along the peeling boundary. Since this range of density brackets the pedestal density needed to achieve ITER's Q=10 mission, the calculation predicts that ITER will operate with pedestal parameters in the range that allow QH-mode operation in present devices.

The second key question is whether the edge rotational shear required by QH-mode can be created in ITER. One part of the answer to that question requires the development of low torque startup scenarios in present machines which lead to shots with edge counter rotation. A final answer to that question requires a validated model of the edge rotation which must include a validated model of the NTV torque. The existence of the NTV torque from NRMF discussed in the present paper gives us a new tool for manipulating the edge rotational shear in ITER while still maintaining co-I_p neutral beam injection.

5. Conclusions

The present results demonstrate that QH-mode sustained by NTV torque from non-axisymmetric magnetic fields created with a coil outside the toroidal coil is a promising operating mode for future burning plasmas including ITER. Using NTV torque to replace counter-I_p NBI torque, we have achieved long duration, counter-rotating QH-mode operation with co-I_p NBI torque up to about 1 Nm. This co-I_p torque is about 3 times the scaled torque that ITER will have. Operation at zero net NBI torque, applicable to RF wave heated plasmas, has also been demonstrated. These experiments utilized an ITER-relevant lower single-null plasma shape and were done with ITER-relevant values ν^*_{ped}~0.05, β^{ped}_T~1% and β_N=2. These discharges exhibited confinement quality H_{98y2}=1.3, in the range required for ITER. Preliminary low q_{95}=3.4 QH-mode plasmas reached fusion gain values of G=0.4, which is the desired value for ITER; the limits on G have not yet been established. The QH-mode work to date has made significant contact with theory. The importance of edge rotational shear is consistent with peeling-ballooning mode theory. We have seen qualitative and quantitative agreement with the predicted NTV torque.

This work was supported by the U.S. Department of Energy under DE-FC02-04ER54698, DE-AC02-09CH11466, DE-AC52-07NA27344, and DE-FG02-05ER54809.

References

[1] GAROFALO, A.M., et al., Nucl. Fusion **51** (2011) 083018.
[2] BURRELL, K.H., et al., Phys. Plasmas **19** (2012) 056117.
[3] BURRELL, K.H., et al. Phys. Plasmas **12** (2005) 056121.
[4] BURRELL, K.H., et al. Nucl. Fusion **49** (2009) 085024.
[5] BURRELL, K.H., et al., Bull. Am. Phys. Soc. **44** (1999) 127.
[6] BURRELL, K.H., et al., Phys. Plasmas **8** (2001) 2153.
[7] SUTTROP, W., et al., Plasma Phys. Control. Fusion **45** (2003) 1399.
[8] SUTTROP, W., et al., Nucl. Fusion **45** (2005) 721.
[9] SAKAMOTO, Y., et al., Plasma Phys. Control. Fusion **46** (2004) A299.
[10] OYAMA, N., et al., Nucl. Fusion **45** (2005) 871.
[11] WEST, W.P., et al., Nucl. Fusion **45**, 1708 (2005).
[12] SCHMITZ, O., et al., Phys. Rev. Lett. **103** (2009) 165005.
[13] FENSTERMACHER, M.E. et al, Phys. Plasmas **15** (2008) 056122.
[14] MAINGI, R., et al., Phys. Rev. Lett. **107** (2011) 145004.
[15] OSBORNE, T.H., et al., J. Physics: Conference Series **123** (2008) 012014.
[16] BURRELL, K.H., et al., Phys. Rev. Lett. **102** (2009) 155993.
[17] SNYDER, P.B., et al., Nucl. Fusion **47** (2007) 961.
[18] PARK, J.-K., et al., Phys. Plasmas **14** (2007) 052110.
[19] PARK, J.-K., et al., Phys. Rev. Lett. **102** (2009) 065002.
[20] FERRARO, N.M., Phys. Plasmas 19, (2012) 056105.
[21] SHAING, K.C., et al., Phys. Plasmas **15** (2008) 082506.
[22] SHAING, K.C., et al., Plasma Phys. Controlled Fusion **51** (2009) 035009.
[23] COLE, A.J., et al., Phys. Plasmas **18** (2011) 055711.
[24] COLE, A.J., et al., Phys. Rev. Lett. **106** (2011) 225002.
[25] GAROFALO, A.M., et al., Phys. Rev. Lett. **101** (2008) 195005.
[26] SNYDER, P.B., et al., Phys. Plasmas **16** (2009) 056118.
[27] SNYDER, P.B., et al., Phys. Plasmas **12** (2005) 056115.